

MASS LOADING BY PROPLYDS OF AN O-STAR WIND

F. García-Arredondo,

Instituto de Física y Matemáticas
Universidad Michoacana de San Nicolás de Hidalgo, México

S. J. Arthur and W. J. Henney

Instituto de Astronomía
Universidad Nacional Autónoma de México, Campus Morelia, México

Received 2002 February 26; accepted 2002 March 18

RESUMEN

Presentamos simulaciones numéricas dependientes del tiempo en una dimensión del proceso de cargado de masa de un viento estelar de una estrella de alta masa debido a los proplyds. Estas se aplican a la estrella O θ^1 Ori C en la nebulosa de Orión, usando una prescripción realista para la tasa de cargado de masa en base de estudios detallados de los proplyds de Orión. Encontramos efectos dinámicos significativos sobre el viento debido al cargado de masa, los cuales se pueden comparar con pruebas observacionales de la dependencia radial de la presión del viento.

ABSTRACT

We present time-dependent, one-dimensional, numerical simulations of the mass loading of the stellar wind from a high-mass star due to embedded proplyds. The simulations are tailored to the O star θ^1 Ori C in the Orion nebula, using realistic mass-loading rates taken from detailed studies of the Orion proplyds. We find significant dynamical effects on the wind due to the mass loading that can be directly compared with observational probes of the radial dependence of the wind pressure.

Key Words: **HYDRODYNAMICS — H II REGIONS — STARS: FORMATION — STARS: WINDS, OUTFLOWS**

1. INTRODUCTION

One of the closest and best-studied regions of recent high-mass star formation is the Orion Nebula (M42, NGC 1976) and its associated cluster of young stars (O'Dell 2001 and references therein). The Orion Nebula cluster contains about 3500 stars within a projected radius of 2.5 pc (Hillenbrand 1997) and its central region, known as the Trapezium cluster, is very centrally condensed (McCaughrean & Stauffer 1994) with a peak density perhaps as high as 2×10^5 stars pc^{-3} (Henney & Arthur 1998). At the center of the cluster lie the 4 high-mass Trapezium stars, the most massive of which is the O7V star θ^1 Ori C, which dominates the total ionizing luminosity of the cluster. Roughly half of the hundred or so low-mass stars within a radius of 0.1 pc of θ^1 Ori C are proplyds, bright emission line objects caused by the photoevaporation of

the young star's circumstellar disk (Laques & Vidal 1979; O'Dell, Wen, & Hu 1993).

In this paper we investigate the effect on the stellar wind from θ^1 Ori C due to the mixing-in of photoevaporated material from the proplyds. The mass-loss rate from each proplyd is in the range $10^{-7} - 10^{-6} M_{\odot} \text{yr}^{-1}$ (Henney & O'Dell 1999; Henney et al. 2002) which is comparable to the stellar wind mass loss ($\sim 3.5 \times 10^{-7} M_{\odot} \text{yr}^{-1}$, García-Arredondo, Henney, & Arthur 2001), so it is reasonable to suppose that the mass flux from proplyds plays an important rôle in the dynamics of the stellar wind.¹

One of the motivations for the present study is the finding of García-Arredondo et al. 2001 that, in

¹On a larger scale, the proplyd mass loss may also have an effect on the ionization balance and dynamics of the H II region but this is not considered here.

order to explain the positions of the stand-off bowshocks in front of different proplyds, it is necessary that the stellar wind pressure falls more slowly with distance than would be expected. One possible cause of this could be mass loading by the proplyds.

The mass loading of stellar winds has been studied by a variety of authors in different contexts. It was first postulated by Hartquist et al. (1986) for a Wolf-Rayet stellar wind in the clumpy nebula RCW 58 and this situation was later modeled numerically (Arthur, Dyson, & Hartquist 1993; Arthur, Henney, & Dyson 1996). The concept of mass loading has also been applied to the winds in planetary nebulae (Arthur, Dyson, & Hartquist 1994). The general properties of mass-loaded winds, both adiabatic and isothermal, have been studied analytically by Williams & Dyson (1994), Williams, Hartquist, & Dyson (1995), Smith (1996), and most recently by the self-similar solutions of Pittard, Dyson, & Hartquist (2001a), Pittard, Hartquist, & Dyson (2001b). The principal effect of mass loading on a stellar wind is to modify its Mach number. In fact, mass loading can cause supersonic flows to evolve into subsonic flows and vice versa if the mass-loading rate is high enough. Also, mass loading initially heats a flow but once the amount of mass added is significant, it can lead to higher cooling rates.

One shortcoming of most previous studies of mass loading is that the mass-loading rate has not been well-constrained by the observations. However, in the present case, the mass-loss rate from the proplyds is known to high accuracy, so that the Orion Nebula is an excellent laboratory for studying the mass loading process in a stellar wind. The only unknown parameter is the efficiency of the mixing (Cantó & Raga 1991; Arthur & Lizano 1997).

In § 2 of this paper, we derive the mass-loading rate due to the proplyds. The numerical model and its results are presented in § 3 and § 4, respectively. In § 5 we discuss the results in the light of analytical models and apply them to observations of the radial variation in the pressure of θ^1 Ori C's wind.

2. MASS-LOADING RATE

To calculate the mass-loading rate per unit volume (q) due to the proplyds, we need to know both the mass-loss rate of each proplyd and their spatial distribution around the exciting star, θ^1 Ori C. Henney & Arthur (1998) found that the spatial density of proplyds can be approximated by

$$\rho_p(r) = \frac{\rho_0}{(1 + r^2/r_0^2)^\alpha}, \quad (1)$$

where ρ_0 is the central stellar density, r is the distance between θ^1 Ori C and the proplyds and r_0 is the core radius at which the stellar density has fallen to one-half of the central value. By taking a sample at $40''$ of an observed density distribution of low-mass stars in the Trapezium cluster, they found that the best-fit density profile is for the values $r_0 = 8''$ (5.16×10^{16} cm, taking a distance of 430 pc to Orion) and $\rho_0 = 1.9 \times 10^5$ stars pc^{-3} . Projected within the core there are ten proplyds. In equation (1) α is a parameter which is fitted to the spatial distribution of the fraction of low-mass stars which are proplyds. The best fit value is $\alpha = 1.29$ (Henney & Arthur 1998). We have recalculated the peak proplyd density, ρ_0 using a different method (see Figure 1) and find that $\rho_0 = 2.5 \times 10^5$ pc^{-3} fits the data best, a slightly higher value than that favored by Henney & Arthur.

We assume that the mass-loss rate from each proplyds does not depend on its distance from θ^1 Ori C and is given by the mean observed rate (Henney & O'Dell 1999), as corrected by Henney (2001), of $\dot{m}_p \simeq 3 \times 10^{-7}$. There is some evidence for a slow decline of mass-loss rate with distance (Henney et al. 2002, § 5.1) but this would have little effect over the length scales considered here.

Once the mass-loss rate and the spatial density of the proplyds are known, we can obtain the mass-loading rate by multiplying these quantities:

$$q = \frac{q_0}{(1 + r^2/r_0^2)^{1.29}} \text{ g cm}^{-3} \text{ s}^{-1}. \quad (2)$$

Here, the peak mass-loading rate is $q_0 = \dot{m}_p \rho_0$.

Mass loss from the proplyds occurs by photoevaporation. When the photoevaporation flow from the proplyds interacts with the stellar wind from θ^1 Ori C, the shocked proplyd gas forms a thin shell which has a continual input of photoevaporated material. A turbulent mixing layer is formed by the shear between the shell and the stellar wind (García-Arredondo et al. 2001). This layer allows the incorporation of the proplyd photoevaporated material into the stellar wind. The efficiency of this process is unknown, so we use fractions of the proplyd mass-loading rate, $f q$, where $f \leq 1$ represents the efficiency of the mixing process, further discussed in § 5 below.

3. NUMERICAL MODEL

The effects of mass loading a stellar wind have been studied with analytical models, for both adiabatic (Smith 1996) and isothermal flows (Williams et al. 1995). These studies assume a steady state and

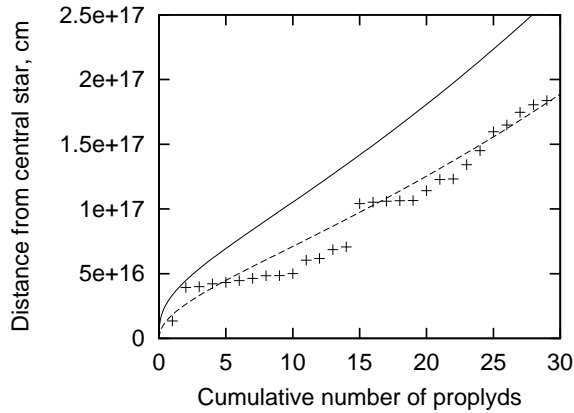


Fig. 1. Distance from central star as a function of cumulative number of proplyds contained within that radius for the proplyd density distribution of equation (1). The solid line shows the true distance while the dashed line shows the projected distance in the plane of the sky. The crosses show the observed projected distances from Bally et al. (1998) for all proplyds within $30''$ of θ^1 Ori C. The theoretical curves correspond to parameters $\rho_0 = 2.5 \times 10^5 \text{ pc}^{-3}$, $r_0 = 5.16 \times 10^{16} \text{ cm}$, $\alpha = 1.29$, and can be seen to reproduce the observed distribution quite well.

do not include explicit heating and cooling. For the mass-loaded winds we wish to model, cooling and heating are important. Furthermore, a steady state is not a good approximation in the shocked stellar wind both because of the heating/cooling and because of the influence that the pressure of the ambient medium has on the mass-loaded wind. For these reasons we must use a numerical model, which we describe below.

3.1. The Equations

The equations to be solved are the time-dependent, one-dimensional, spherically symmetric gas dynamic equations, which in conservation form are

$$\frac{\partial \rho}{\partial t} + \frac{1}{r^2} \frac{\partial}{\partial r} (r^2 \rho u) = q, \quad (3)$$

$$\frac{\partial}{\partial t} (\rho u) + \frac{1}{r^2} \frac{\partial}{\partial r} [r^2 (p + \rho u^2)] = \frac{2p}{r}, \quad (4)$$

$$\frac{\partial E}{\partial t} + \frac{1}{r^2} \frac{\partial}{\partial r} [r^2 u (E + p)] = G - L, \quad (5)$$

where q in the mass-loading rate described in § 2, $E = p/(\gamma - 1) + \rho u^2/2$ is the total energy density, L is the radiative cooling rate per unit volume and G is the heating rate per unit volume. All other symbols have their usual meaning. In this paper we take the cooling rate to be a simple piecewise fit to the radiative cooling curve, with $L = An^2T^{1.1}$ for

temperature $10^4 \leq T \leq 10^5 \text{ K}$, $L = Bn^2T^{-1/2}$ for $10^5 \leq T \leq 10^7 \text{ K}$, and $L = Cn^2T^{1/2}$ for $T > 10^7 \text{ K}$, where A , B , and C are constants with the values 2.38×10^{-27} , 2.38×10^{-19} and 4.76×10^{-27} in cgs units (Arthur et al. 1993). The heating rate is assumed to have the form $G = Dn^2T^{-1/2}$, appropriate for optically thin photoionization heating, with D chosen so that the net heating $G - L$ is zero at $T = 10^4 \text{ K}$.

We use a fourth equation to trace a passive scalar which marks the extent of the stellar wind material on the grid

$$\frac{\partial \epsilon \rho}{\partial t} + \frac{1}{r^2} \frac{\partial}{\partial r} (r^2 \epsilon \rho u) = \epsilon q, \quad (6)$$

where ϵ is the passive scalar, which takes a value of 0 for the stellar wind and 1 for the ambient photoionized medium in this work. Finally we take γ , the ratio of specific heats, to be $5/3$.

3.2. The Model

The hydrodynamic equations are integrated using a second order one-dimensional time-dependent Eulerian Godunov-type code (Godunov 1959) as described by Arthur (1991).

For the stellar wind from θ^1 Ori C we take a terminal stellar wind velocity of $v_* = 1200 \text{ km s}^{-1}$ and a mass-loss rate of $\dot{M}_* = 3.5 \times 10^{-7} M_\odot \text{ yr}^{-1}$ (see e.g., García-Arredondo et al. 2001). At its point of origin the wind has a temperature of 10^4 K .

The stellar wind is assumed to expand into a uniform photoionized medium. In the Orion Nebula the ionized densities measured in different directions from θ^1 Ori C differ by up to 2 orders of magnitude. Towards the molecular cloud the number density is $\sim 10^4 \text{ cm}^{-3}$ (Pogge, Owen, & Atwood 1992) whereas in the directions away from the molecular cloud where the blister of the Orion Nebula is open, the densities are much lower ($n \sim 10^2 - 10^3 \text{ cm}^{-3}$, Subrahmanyan, Goss, & Malin 2001). For this reason, in our models we consider 3 cases with uniform ambient densities of 10^2 , 10^3 and 10^4 cm^{-3} respectively. In all models the temperature in this photoionized ambient medium is taken to be 10^4 K , hence the ambient pressure in each of the three models will be different, varying by 2 orders of magnitude.

We have supposed a spherically symmetric model because we are interested in the inner region of Orion where the stellar wind of θ^1 Ori C is supersonic. Although the Orion Nebula is not spherically symmetric, the stellar wind is approximately so in the region of our interest. We ignore the complexities brought

on by the fact that the H II region is a champagne flow, and that on one side the stellar wind will be interacting with a transonic flow away from the principal ionization front. These complications should have a minimal effect on the inner regions of the stellar wind.

3.3. Numerical Diffusion

The swept-up ambient medium material and the shocked stellar wind are separated by a contact discontinuity. There are around 3 orders of magnitude difference in density between the two sides. Since the grid resolution is finite, truncation errors lead to numerical diffusion, which means that the shocked stellar wind and the swept-up ambient medium will be mixed in the cells closest to the contact discontinuity. As a result, there will be overcooling in the shocked stellar wind close to the discontinuity. This, in turn, leads to acoustic waves reflecting off internal flow structure producing oscillations in the flow variable distributions.

This problem can be resolved by finding the cells in which the cooling is more than double the cooling in its neighbours and then limiting the cooling in these cells (Stone & Norman 1993). Another possible solution is to make use of the passive scalar label and turn off the cooling in the stellar wind material that is close to the contact discontinuity (Mac Low & Ferrara 1999; Yabe & Xiao 1993).

In this paper we have used a combination of these two methods in our simulations. We find that, for the passive scalar values 0 (wind) and 1 (ambient medium), turning off the cooling in the range 0.7–0.9 and also imposing an upper limit on the cells with overcooling which was double the average of the neighbouring cells made the numerical diffusion problem disappear almost completely. When the density in the ambient medium is low ($< 10^3 \text{ cm}^{-3}$) the numerical diffusion almost disappears because the differences in density between the two sides of the contact discontinuity are not very high.

4. RESULTS OF THE SIMULATIONS

Figures 2, 3 and 4 show the results for mass-loading efficiency factors $f = 0.0$, 0.1 , and 1.0 , respectively. Each figure shows temperature, density and Mach number as function of radius. The different curves represent different values of the ambient density $n = 10^4$, 10^3 and 10^2 cm^{-3} . All the results correspond to a total elapsed time of $\sim 140,000$ yrs since the onset of the stellar wind. This is close to the probable age of θ^1 Ori C (Palla & Stahler 2001; Henney et al. 2002). Moreover, this time is sufficient

for the inner parts of the flow to become stationary. In each figure only the inner region of the numerical grid is shown, which corresponds approximately to the size of the Orion Nebula.

The high densities in the ambient medium mean that the swept up shell cools rapidly. The outer shock degenerates into a sound wave in a time $\simeq 40,000(n/10^3 \text{ cm}^{-3})^{-1/2}$ years (Dyson & Williams 1997), so the pressures in the shocked stellar wind material and ambient medium are roughly equal. The position of the global stellar wind shock depends on the ambient density because it is determined by the balance of the preshock ram pressure and the ambient pressure. Therefore, lower ambient densities (and thus pressures) imply that the shock is further from the star. This is clearly seen in Fig 2, which corresponds to the case of no mass loading.

The effects of mass loading are very notable in the figures. Firstly, the size of the stellar wind bubble is reduced. A high mass-loading factor ($f = 1$) can lead to cooling in the shocked stellar wind and therefore reduces its pressure. For zero and low ($f = 0.1$) mass-loading rates, the shocked stellar wind does not cool efficiently and a hot bubble results.

When the mass-loading rate is high ($f = 1.0$), the stellar wind has a sonic point at the edge of the core region, after which the flow accelerates again, becoming supersonic on leaving the core and leads to the formation of a shock. When the ambient density is high ($n = 10^4 \text{ cm}^{-3}$) this shock is weak (see Fig. 4) but for lower ambient pressures the transonic mass-loaded flow accelerates further and shocks at a higher Mach number. In the zero and low mass-loading cases the stellar wind passes through a global shock. For high ambient densities the global shocks for the $f = 0$ and $f = 0.1$ cases are coincident but for lower ambient densities they become spatially separated. Mass loading enhances the density in the stellar wind at all radii outside the core region.

The spikes in the Mach number and temperature plots at the position of the contact discontinuity between the shocked stellar wind and the swept up ambient medium are numerical artefacts caused by the numerical diffusion problem mentioned in § 3. The oscillations in Fig. 2 are due to this same problem. If we had not taken the steps outlined in § 3, the oscillations would be much bigger.

5. DISCUSSION

In order to understand the behavior of our flow solutions, we can use the results of previous analytic studies that have considered a spatial variation in the mass-loading rate similar to ours. Williams & Dyson

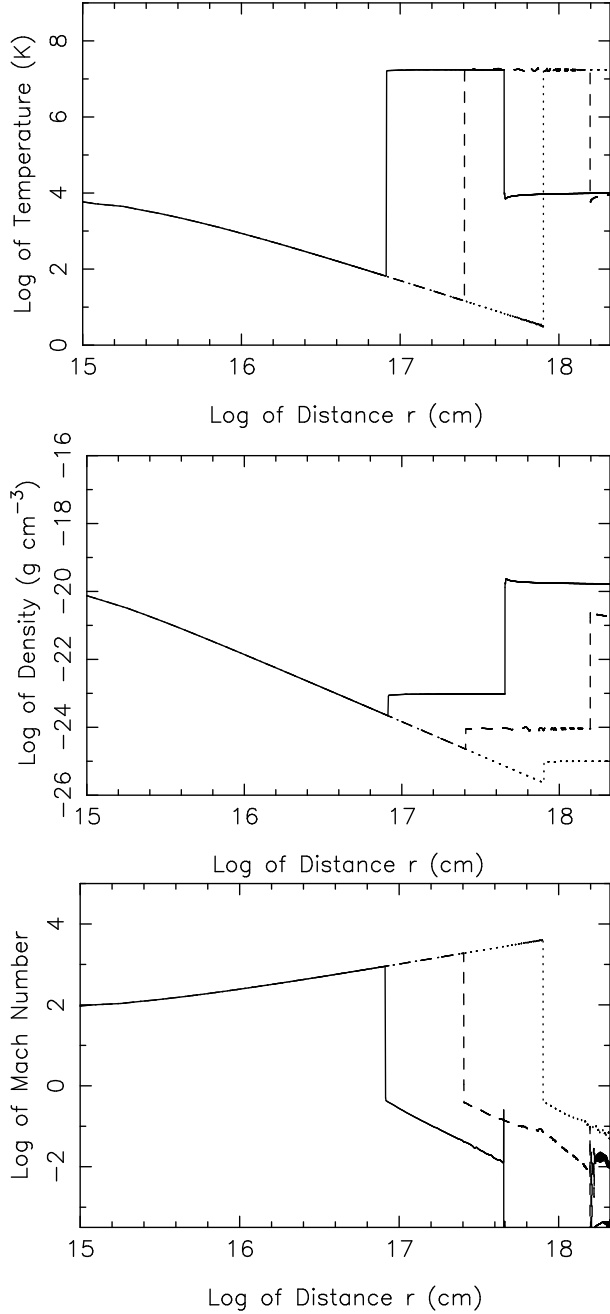


Fig. 2. Results of the numerical model without mass loading. Log of temperature is the upper panel, log of density is the middle panel and log of Mach number is the lower panel. Solid line for $n = 10^4 \text{ cm}^{-3}$, dashed line for $n = 10^3 \text{ cm}^{-3}$ and dotted line for $n = 10^2 \text{ cm}^{-3}$.

(1994) studied the effect of a finite region of uniform mass loading on an initially subsonic isothermal flow, finding that the flow becomes supersonic at the core radius. Smith (1996) considered the case of an adiabatic, initially supersonic, mass-loaded wind where the mass-loading function is similar to ours. The po-

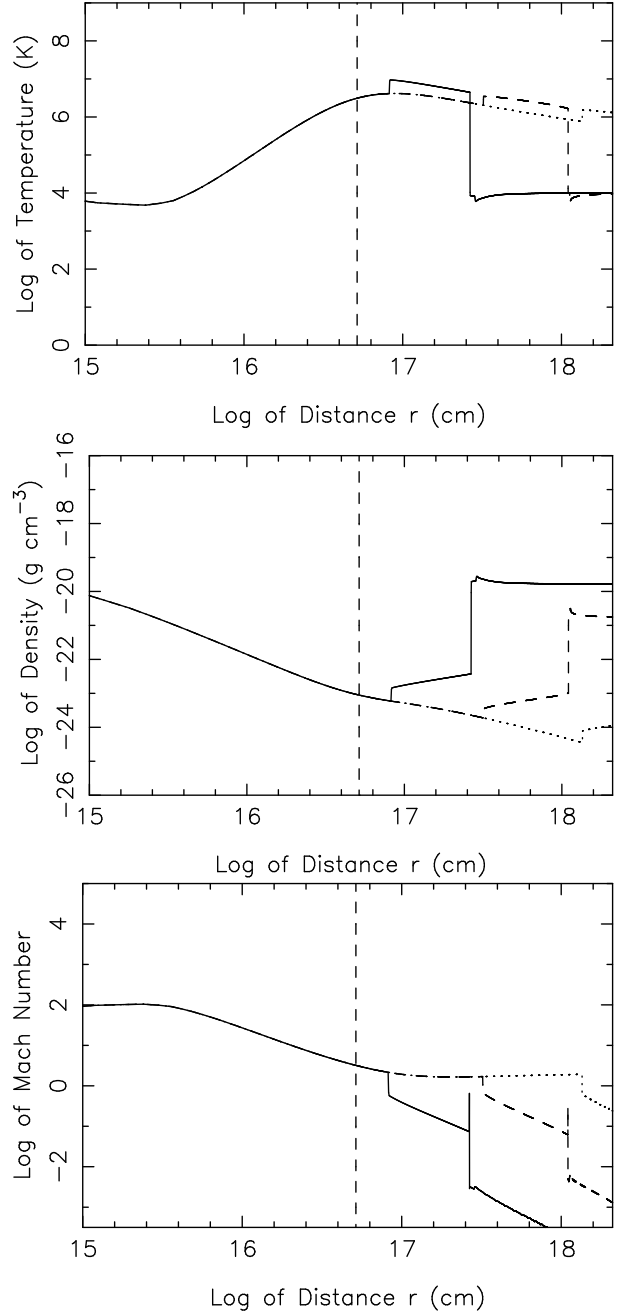


Fig. 3. Same as the Fig 2 but with $f = 0.1$. The vertical dashed line represents the core radius.

sition of the sonic point is determined by the ratio of the mass-loss rate in the stellar wind to that due to the mass loading. A simple estimate can be made by considering the following equation for the Mach number (Smith 1996).

$$\frac{1}{M^2} \frac{dM^2}{dr} = 2 \frac{[(\gamma - 1)M^2 + 2][\dot{m} - (\gamma M^2 + 1)\pi r^3 q]}{(M^2 - 1)\dot{m}r}. \quad (7)$$

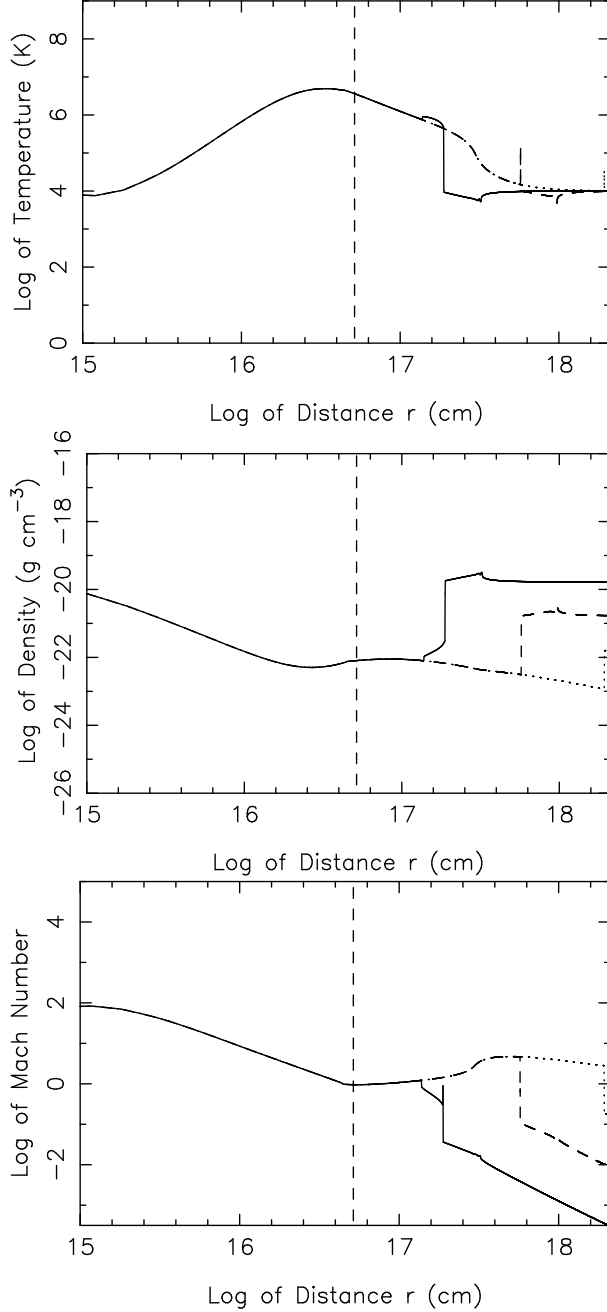


Fig. 4. Same as Fig 3 but with $f = 1.0$.

This equation is obtained by combining equations (3), (4) and (5) in the adiabatic and stationary case (which corresponds to the situation in the unshocked stellar wind) and with the definitions $M = u/c$, $c^2 = \gamma p/\rho$ and $\dot{m} = \dot{M}_* + 4\pi \int qr^2 dr$. For the derivative of the Mach number to pass smoothly through the sonic point ($M = 1$) we require

$$\dot{m} - (\gamma + 1)\pi r^3 q = 0, \quad (8)$$

and taking the approximation $q = f\dot{m}_p\rho_0$ in the core we find the position of the sonic point be

$$r_s = \left[\frac{3\dot{M}_*}{4\pi f\dot{m}_p\rho_0} \right]^{1/3}. \quad (9)$$

For the sonic point to occur within the core we require $r_s < r_0$, which, for the values given in § 2, implies that the mass-loading efficiency must be greater than a critical value: $f > f_{\text{crit}} \simeq 0.216$. Outside of the core region the mass-loading rate falls as $r^{-2.58}$, which gives a supersonic solution that shocks at a radius depending on the external pressure. This simple analytical estimate is consistent with the results of our numerical simulations: our $f = 1.0$ case (Fig. 4) does pass through a sonic transition within the core, while our $f = 0.1$ case (Fig. 3) does not.

One of the motivations for the present work comes from García-Arredondo et al. (2001) who modeled the interaction between the stellar wind from θ^1 Ori C and the photoevaporated flow from a proplyd and compared the results with observations of the bowshocks seen in front of many proplyds. They found that in most cases the position of the bowshock could be found by simple ram pressure balance between the stellar wind and the photoevaporated flow. However, in the farthest two of the studied cases, the proplyd ram pressure was higher than that expected from a supersonic stellar wind (see García-Arredondo et al. 2001, Figure 2). García-Arredondo et al. attempted to resolve the problem by positing that the farther proplyds lay in the shocked subsonic region of the stellar wind. However, in these simulations the shell of shocked photoevaporated flow material grew too thick and the eddies in the shear layer did not disperse quickly enough. It was concluded that a higher Mach number flow was required. A pure stellar wind can not provide the necessary hydrodynamic conditions and so it was suggested that mass loading due to the inner proplyds could modify the flow sufficiently to give the required pressure at the position of 177-341.

Figure 5 shows the total pressure in the mass-loaded wind as a function of projected radius for the model with $n = 10^3 \text{ cm}^{-3}$. In this figure we show the results for each of the cases $f = 0$, $f = 0.1$ and $f = 1.0$. Also plotted on the figure are the points corresponding to the proplyds 167–317 and 177–341. The proplyd 167–317 has a well determined inclination angle of 50° (Henney et al. 2002) and each panel of the figure shows the curves that correspond to the mass-loaded stellar wind pressure projected at 50° and 90° (which is close to the estimated angle

for 177–341). The observational uncertainties in the proplyd ram pressures are of order 10% (see García-Arredondo et al. 2001) and are indicated by 1σ error bars in the figure.

From the upper panel, it is apparent that a supersonic wind without mass loading is incapable of providing enough ram pressure at the position of 177–341 to maintain the standoff bowshock in its observed position, as was pointed out by García-Arredondo et al. (2001). However, the middle panel shows that our $f = 0.1$, $n = 10^3 \text{ cm}^{-3}$ mass-loaded model fits the observations very well. For this model, the wind properties at small radii are little changed from the no-mass-loading case, but outside the core radius, r_0 , the flow is only somewhat supersonic and the total (ram plus thermal) pressure is increased by a factor of about 50%. For our $f = 1.0$ model, the flow is approximately sonic throughout the distance range of interest and the predicted pressure is uniformly too high.

The required mixing efficiency of $f = 0.1$ would seem to be somewhat high if one only considered the mixing at the surface of a single proplyd bowshock. However, each bowshock wake subtends a significant solid angle as seen from θ^1 Ori C and so the wakes will begin to overlap and interact with one another, greatly increasing the efficiency of the mixing. If the asymptotic half opening angle of the bowshock wake is θ_∞ (see Cantó, Raga, & Wilkin 1996), then the corresponding solid angle is $\Omega_b = 2\pi(1 - \cos\theta_\infty)$. Assuming no clustering and an isotropic distribution of proplyds with respect to the central star, then the total fraction of the full 4π steradians covered by wakes at a given distance, r , is $f_{\text{tot}} = 1 - (1 - \Omega_b/4\pi)^{N(r)}$, where $N(r)$ is the number of proplyds with distances less than r (see Fig. 1). This fraction is plotted in Figure 6. Significant interactions between wakes will occur for $f_{\text{tot}} > 0.5$ and this can be seen to occur just outside the core radius, at $r \simeq 6 \times 10^{16} \text{ cm}$. At the position of 177–341, f_{tot} is around 90%, so a mixing efficiency of 10% does not seem unreasonable.

This efficiency is really that for reasonably prompt mixing, that is, within a fraction of a core radius of the proplyd position. If the flow is followed sufficiently far downstream, then all the proplyd material should mix in to the flow eventually. However, taking account of this would substantially complicate our calculations since the radial distribution of mass injection would no longer necessarily follow that of the proplyds. This would only have an important effect on the results if it managed to substantially flatten the mass injection distribution, so that the radial power law were less steep than -1.5

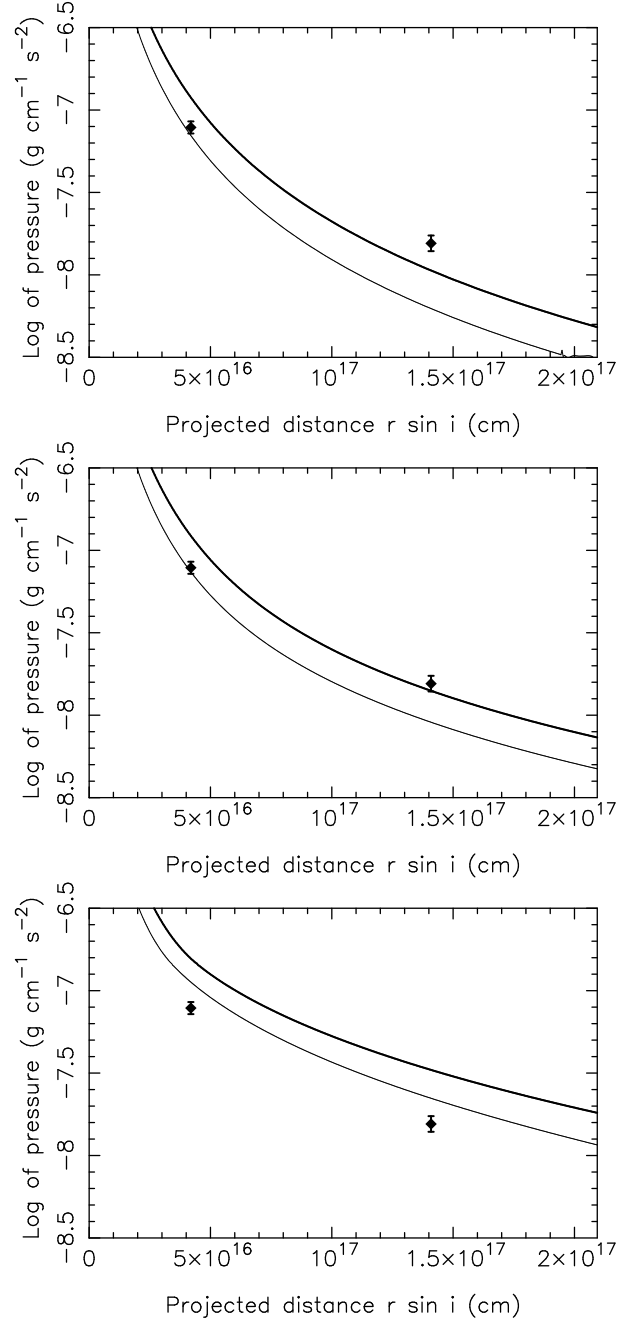


Fig. 5. Total pressure vs projected distance ($r \sin i$), where i is the proplyd inclination angle. The thicker lines correspond to an inclination angle of 90° and thinner lines are for $i = 50^\circ$. The panels, top, middle and lower are the plots for $f = 0$, $f = 0.1$ and $f = 1$ respectively. All plots are with an ambient density of $n = 10^3 \text{ cm}^{-3}$. The diamonds are ram pressure of the proplyd photoevaporated flows at the position of their respective stand-off shocks.

outside the core (Smith 1996). A fully satisfactory treatment of the mixing process would require much

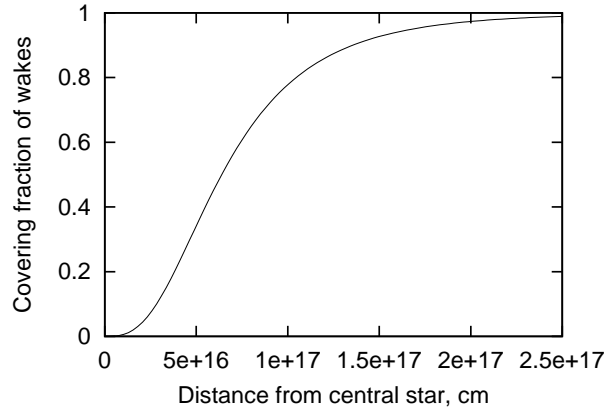


Fig. 6. Cumulative area covering fraction of bowshock wakes as a function of distance from θ^1 Ori C. For simplicity, each bowshock is assumed to have an asymptotic half opening angle of 45° .

greater computational resources than are currently available.

Since the spatial scale at which effects of mass loading become important is comparable to the separation between the high-mass stars of the Trapezium, then it might be thought that an alternative resolution of the apparent pressure discrepancy discussed above could be that the winds from stars other than θ^1 Ori C become important at the larger scales. However, the next earliest stars in the central Trapezium after θ^1 Ori C (O7V) are θ^1 Ori A and θ^1 Ori D, both of which are of spectral type B0.5V (Levato & Abt 1976) and hence have bolometric luminosities that are 6–8 times smaller than θ^1 Ori C. Standard correlations between wind strength and stellar parameters for OB stars (Lamers & Cassinelli 1999) give wind momentum fluxes for these two stars that are only 2–4% that of θ^1 Ori C. Hence, neither will make a significant contribution apart from in a small volume close to the star itself.

6. CONCLUSIONS

In this paper we have presented a numerical hydrodynamic model for the mass loading of the stellar wind from a high-mass star due to embedded proplyds. We have applied this model to the Orion nebula proplyds that are immersed in the wind from θ^1 Ori C. We find that for reasonable values of the mixing efficiency the dynamic effects are significant. In particular, the wind undergoes considerable heating while it is still supersonic and its total pressure (ram plus thermal) falls more slowly with distance than in the case of a non-mass-loaded wind. For higher values of the mass-loading rate than are prob-

ably appropriate in Orion, the wind can be driven to a sonic point at the edge of the mass-loading core.

We find that mass loading of θ^1 Ori C's wind allows the standoff bowshocks of the farther proplyds discussed by García-Arredondo et al. (2001) to be in pressure balance with the stellar wind without having to postulate that it has first passed through a global shock. This is a much more satisfactory explanation for the appearance of the bowshock in 177–341 than that offered by García-Arredondo et al.

As perhaps the best-observed of all astronomical objects outside the Solar System, the inner Orion nebula provides an excellent laboratory for the study of the mass loading. The meso-scale process of mass injection from the proplyds is well-characterized both observationally and theoretically. Furthermore, even subtle variations in the stellar wind properties can be compared against observational probes. As well as the dynamical effects on the stellar wind, the mass loading from the proplyds may also have ionization and dynamical effects on the larger-scale champagne flow of the nebula, as first pointed out to us by D. Hollenbach (1998 priv. comm.).

We thank R. Williams for useful discussions about numerical diffusion and G. Mellema for pointing out the potential influence of the winds from the other Trapezium stars. We also thank the referee, J. Dyson, for a helpful and insightful report. FGA is grateful to CONACyT, México for a student scholarship. We acknowledge support from projects DGAPA-PAPIIT IN117799 (UNAM, México) and 37250-E (CONACyT, México).

REFERENCES

- Arthur, S. J. 1991, PhD thesis, University of Leeds
 Arthur, S. J., Dyson, J. E., & Hartquist, T. W. 1993, MNRAS, 261, 425
 ———. 1994, MNRAS, 269, 1117
 Arthur, S. J., Henney, W. J., & Dyson, J. E. 1996, A&A, 313, 897
 Arthur, S. J., & Lizano, S. 1997, ApJ, 484, 810
 Cantó, J., & Raga, A. C. 1991, ApJ, 372, 646
 Cantó, J., Raga, A. C., & Wilkin, F. P. 1996, ApJ, 469, 729
 Dyson, J. E., & Williams, D. A. 1997, *The Physics of the Interstellar Medium*, 2nd Ed. (Bristol, UK: IOP)
 García-Arredondo, F., Henney, W. J., & Arthur, S. J. 2001, ApJ, 561, 830

- Godunov, S. K. 1959, *Mat. Sb.*, 47, 271
- Hartquist, T. W., Dyson, J. E., Pettini, M., & Smith, L. J. 1986, *MNRAS*, 221, 715
- Henney, W. J. 2001, in *RevMexAASC 10, The Seventh Texas-Mexico Conference on Astrophysics: Flows, Blows and Glows*, eds. W. H. Lee & S. Torres-Peimbert (México, D. F.: Inst. Astron., UNAM), 57
- Henney, W. J., & Arthur, S. J. 1998, *AJ*, 116, 322
- Henney, W. J., & O'Dell, C. R. 1999, *AJ*, 118, 2350
- Henney, W. J., O'Dell, C. R., Meaburn, J. Garrington, S. T., & Lopez, J. A. 2002, *ApJ*, 566, 315
- Hillenbrand, L. A. 1997, *AJ*, 113, 1733
- Lamers, H. J. G. L. M., & Cassinelli, J. P. 1999, *Introduction to Stellar Winds* (Cambridge, UK: CUP)
- Laques, P., & Vidal, J. P. 1979, *A&A*, 73, 97
- Levato, H., & Abt, H. A. 1976, *PASP*, 88, 712
- Mac Low, M.-M., & Ferrara, A. 1999, *ApJ*, 513, 142
- McCaughrean, M., & Stauffer, J. 1994, *AJ*, 108, 1328
- O'Dell, C. R. 2001, *ARA&A*, 39, 990
- O'Dell, C. R., Wen, Z., & Hu, X. 1993, *ApJ*, 410, 696
- Palla, F., & Stahler, S. W. 2001, *ApJ*, 553, 229
- Pittard, J. M., Dyson, J. E., & Hartquist, T. W. 2001a, *A&A*, 373, 1043
- Pittard, J. M., Hartquist, T. W., & Dyson, J. E. 2001b, *A&A*, 373, 1043
- Pogge, R. W., Owen, J. M., & Atwood, B. 1992, *ApJ*, 399, 147
- Smith, S. J. 1996, *ApJ*, 473, 773
- Stone, J. M., & Norman, M. L. 1993, *ApJ*, 413, 198
- Subrahmanyam, R., Goss, W. M., & Malin, D. F. 2001, *ApJ*, 121, 399
- Williams, R. J. R., & Dyson, J. E. 1994, *MNRAS*, 270, L52
- Williams, R. J. R., Hartquist, T. W., & Dyson, J. E. 1995, *ApJ*, 446, 759
- Yabe, T., & Xiao, F. 1993, *J. Phys. Soc. Japan*, 62, 2537

S. Jane Arthur and William J. Henney: Instituto de Astronomía, UNAM, Apartado Postal 3-72, 58090 Morelia, Michoacán, México (j.arthur,w.henney@astrosmo.unam.mx).

Fulgencio García-Arredondo: Instituto de Física y Matemáticas, Universidad Michoacana de San Nicolás de Hidalgo, Apartado Postal 2-82, 58040 Morelia, Michoacán, México (f.garcia@astrosmo.unam.mx).